Separation Science and Technology
Publication details, including instructions for authors and subscription information:
http://www.informaworld.com/smpp/title~content=t713708471

SEPARATIONS BASED ON MAGNETOPHORETIC MOBILITY

Maciej Zborowski[a]; Lee R. Moore[a]; P. Stephen Williams[a]; Jeffrey J. Chalmers[b]
[a] Department of Biomedical Engineering/ND20, The Cleveland Clinic Foundation, Cleveland, OH, U.S.A. [b] Department of Chemical Engineering, The Ohio State University, Columbus, OH, U.S.A.

Online publication date: 12 February 2002

MARCEL DEKKER, INC. • 270 MADISON AVENUE • NEW YORK, NY 10016

SEPARATION SCIENCE AND TECHNOLOGY
Vol. 37, No. 16, pp. 3611–3633, 2002

SEPARATIONS BASED ON MAGNETOPHORETIC MOBILITY

Maciej Zborowski,[1,*] Lee R. Moore,[1] P. Stephen Williams,[1] and Jeffrey J. Chalmers[2]

[1]Department of Biomedical Engineering/ND20, The Cleveland Clinic Foundation, 9500 Euclid Avenue, Cleveland, OH 44195
[2]Department of Chemical Engineering, The Ohio State University, 140 East 19th Street, Columbus, OH 43210

ABSTRACT

Magnetophoretic mobility arises from the motion of an electrically neutral body in a viscous medium when exposed to an inhomogenous magnetic field. Conforming to other types of mobility, which generally have the form of a "reciprocal friction coefficient" (such as electrophoretic mobility), we have defined the magnetophoretic mobility, m, as a ratio of a particle–field interaction parameter, ϕ_m, to the particle friction coefficient, f, so that $m = \phi_m/f$, with the parameter ϕ_m equal to the product of the magnetic susceptibility of the particle relative to that of the medium, $\Delta\chi$, and its volume, V_m, so that $\phi_m = \Delta\chi V_m$. The particle mobility is an important factor in predicting separation when a mixture of particles of different mobilities is exposed to an external

*Corresponding author. Fax: (216) 444-9198; E-mail: zborow@bme.ri.ccf.org

DOI: 10.1081/SS-120014809
0149-6395 (Print); 1520-5754 (Online)

www.dekker.com

field. We have combined the information about the particle magnetophoretic mobility, measured by cell tracking velocimetry, and the theory of the split-flow thin channel fractionation, to describe particle and cell separations in a flowing solution through an annular channel coaxial with a quadrupole magnetic field. The theoretical model was verified by experiments with monodisperse magnetic polymeric particles and human white blood cells.

Key Words: Magnetophoresis; Magnetic mobility; Cell separation; Cell tracking; Velocimetry; Antibody binding capacity

INTRODUCTION

Magnetophoresis is the process of particle motion in a viscous medium under the influence of the magnetic field.[1–6] Here we assume that the dimensions of the particles undergoing magnetophoresis are limited to the range $1-100\,\mu$m, and their electrical conductivity is negligible (the particles are dielectric). Because of those limitations, the effects of Brownian motion and the electric current induction due to motion in the magnetic field can be disregarded. The imposed magnetic field is considered constant in the time domain (magnetostatic) and variable in the spatial domain (inhomogenous or nonuniform field). The processes of magnetophoresis are governed by the laws of magnetoquasistatics (as described by Melcher[7]). The magnetic particles and the medium are considered responsive to the imposed magnetic field, and the material property that describes the response to the external magnetic field is the relative magnetic permeability, μ, and the magnetic susceptibility, χ (defined later). A characteristic property of the magnetic field is that it is source-free (solenoidal), which is a consequence of the experimental fact that no magnetic monopoles (or magnetic charges) have been detected to date. The magnetic particle in the imposed magnetic field behaves as a magnetic dipole. In a uniform magnetic field the net force on the magnetic dipole is zero, and there is no translational motion of the magnetic particle (although there may be a rotational motion due to the torque exerted by the field on the dipole). To cause the translational motion of a magnetic particle, a nonuniform magnetic field is necessary, with both the field magnitude and the field gradient playing a role. The characteristic property of the magnetic particle that causes it to move in a nonuniform magnetic field is defined as its magnetophoretic mobility, m.

The difference in magnetophoretic mobility between different particles establishes a basis for magnetic separation in viscous media. If such a particle property could be measured, the particle magnetophoretic mobility would become an important parameter for a rational magnetic separator design. In particular,

development of a magnetic separator based on the transport—rather than equilibrium—process would become possible. The advantage of the transport over the equilibrium mode separations is higher throughput, scalability, and a gentler separation process, which make it particularly appealing to biological separations. Magnetic separations became popular in biological and medical sciences due to an increase in availability of antibodies and magnetic reagents suitable for cell magnetization, and a relatively uncomplicated separation process.[8–10] The current, commercial magnetic cell separators operate in the equilibrium mode, characterized by precipitation of the magnetic material on a solid support when exposed to the magnetic field, which is suboptimal. We set out to design, build, and evaluate an instrument for particle magnetophoretic mobility measurement, and to construct a magnetic cell sorter for operation on the basis of differential particle mobilities in continuously flowing solution. Here we summarize the theoretical and experimental basis for cell separation based on differential cell magnetophoretic mobilities.

THEORY

A remarkable property of the electromagnetic field is summarized in Thomson's theorem (specialized here to the magnetic field, as adapted from Becker[11]): when the dipoles in a magnetostatic field move under the influence of the field, the energy of the field diminishes by the quantity of the available work. The dipoles will therefore, so far as they are free to move, seek to arrange themselves in such a way that the field energy will have the least possible value. In other words, when describing the system in terms of the thermodynamic quantities, the field energy is equivalent to Gibbs free energy, G:

$$G = -p_{\mathrm{m}}B \tag{1}$$

where p_{m} is the magnetic moment and B is the imposed magnetic field induction. The magnetophoretic processes considered here occur under isothermal conditions, and therefore the work performed on the magnetic dipole equals the change in the Gibbs energy:

$$\mathrm{d}W = \mathrm{d}G \tag{2}$$

The incremental mechanical work expended by the field on moving the dipole against the viscous forces is that part of the Gibbs free energy change which is not involved in the particle magnetization, $\mathrm{d}G' = -B\,\mathrm{d}p_{\mathrm{m}}$. Assuming that the processes involved in the dipole motion in the magnetic field are reversible, the potential energy of the system, U, can be defined:

$$\mathrm{d}U \equiv \mathrm{d}W - \mathrm{d}G' = \mathrm{d}G - (-B\,\mathrm{d}p_{\mathrm{m}}) = -p_{\mathrm{m}}\,\mathrm{d}B - B\,\mathrm{d}p_{\mathrm{m}} + B\,\mathrm{d}p_{\mathrm{m}}$$

$$= -p_{\mathrm{m}}\mathrm{d}B \tag{3}$$

The resultant force acting on the magnetic dipole is the negative gradient of the potential energy.[12] For a freely suspended magnetic dipole one obtains:

$$\begin{cases} \mathrm{d}U = -p_{\mathrm{m}}\,\mathrm{d}B \\ \mathbf{F} = -\frac{\mathrm{d}U}{\mathrm{d}\mathbf{r}} = p_{\mathrm{m}}\frac{\mathrm{d}B}{\mathrm{d}\mathbf{r}} \equiv p_{\mathrm{m}}\nabla B \end{cases} \tag{4}$$

where ∇ is the nabla operator, $\nabla \equiv [\partial/\partial x, \partial/\partial y, \partial/\partial z] \equiv \mathrm{d}/\mathrm{d}\mathbf{r}$, which produces a vector when acting on a scalar quantity (here, the magnitude of the magnetic field, B). The magnetic field is fully described by the three vectors, **B**, the field induction, **H**, the field strength, and **M**, the magnetization of the medium, where the following relationships hold:

$$\begin{cases} \mathbf{B} = \mu\mu_0\mathbf{H} \\ \mathbf{M} \equiv \frac{\mathbf{B}}{\mu_0} - \mathbf{H} = \chi\mathbf{H} \\ \mu = 1 + \chi \end{cases} \tag{5}$$

Here μ (the permeability) and χ (the susceptibility) are the material parameters (which may or may not depend on the field strength, H), and μ_0 is the magnetic permeability of free space. The vector quantities are indicated by bold type.

In defining the magnetophoretic mobility, m, we follow the heuristic approach characteristic of all definitions pertaining to material constants, namely, we require that it is independent of the field for linear systems, and then assume that it remains valid even in modeling systems, which are nonlinear with regard to the field parameters (see, for example, the discussion by Melcher in Ref. [13]). Therefore, we require that the magnetophoretic mobility depends on the particle and solution parameters but not on the imposed field, for a system for which the following condition holds:

$$\chi = \text{const.} \tag{6}$$

which is characteristic of linearly polarizable media. For a particle of susceptibility χ_{p}, immersed in a continuous medium (fluid) of the susceptibility χ_{f}, the requirement of a linear polarization of both the particle and the medium leads to:

$$\Delta\chi = \chi_{\mathrm{p}} - \chi_{\mathrm{f}} = \text{const.} \tag{7}$$

Therefore, the magnetic quantities of the particle relative to those of the continuous medium obey the following relationships:

$$\Delta p_{\mathrm{m}} = \Delta M V_{\mathrm{m}} = \Delta\chi H V_{\mathrm{m}} \equiv \phi_{\mathrm{m}} H = \phi_{\mathrm{m}}\frac{B}{\mu_0} \tag{8}$$

where V_{m} is the volume of the magnetic particle, and here we introduced "the particle–field interaction parameter," $\phi_{\mathrm{m}} \equiv \Delta\chi V_{\mathrm{m}}$. Such a parameter has been

defined in the separation sciences as a proportionality factor between the force acting on a particle and the force field strength.[14–17] Upon insertion of the last expression into the expression for the magnetic force, **F**, stated earlier, one obtains:

$$\mathbf{F} = \Delta p_{\mathrm{m}} \nabla B = \phi_{\mathrm{m}} \nabla \left(\frac{B^2}{2\mu_0} \right) \tag{9}$$

where the use was made of the fact that the magnetostatic field is irrotational and therefore $\nabla B^2 = 2B\nabla B$. The quantity in the parentheses equals the magnetic field energy density in the air, i.e., outside the medium, in which the separation takes place ($\mu \approx 1$ for air). Note that the force direction depends on the sign of ϕ_{m}: the force is directed towards the increasing magnetic field for $\phi_{\mathrm{m}} > 0$ (paramagnetic effects), and away from the increasing magnetic field for $\phi_{\mathrm{m}} < 0$ (for a review of diamagnetic effects in strong fields, see Ref. [18]). The magnetic force on the dipole is opposed by the viscous drag, which for quasistatic processes leads to the following equation:

$$\mathbf{F} - f\mathbf{u}_{\mathrm{m}} = \phi_{\mathrm{m}} \nabla \left(\frac{B^2}{2\mu_0} \right) - f\mathbf{u}_{\mathrm{m}} = 0 \tag{10}$$

and therefore

$$\mathbf{u}_{\mathrm{m}} = \frac{\phi_{\mathrm{m}}}{f} \nabla \left(\frac{B^2}{2\mu_0} \right) \tag{11}$$

where $\mathbf{u}_{\mathrm{m}}$ is the magnetic dipole velocity in the viscous medium and f is the friction coefficient ($f = 3\pi\eta D_{\mathrm{c}}$ for Stokes regime, where η is the fluid viscosity and D_{c} is the magnetized particle diameter). In the high-gradient magnetic separation (HGMS) literature, $\mathbf{u}_{\mathrm{m}}$ is known as "the magnetic drift velocity."[19–21]

The right-hand side of the last equation has the desired feature of being a product of strictly particle and viscous medium properties, ϕ_{m}/f, and the magnetic field property, $\nabla(B^2/2\mu_0)$, which suggest the following separation of variables:

$$m \equiv \frac{\phi_{\mathrm{m}}}{f} = \frac{\Delta\chi V_{\mathrm{m}}}{f} \tag{12}$$

and

$$\mathbf{S}_{\mathrm{m}} \equiv \nabla \left(\frac{B^2}{2\mu_0} \right) \tag{13}$$

so that the expression for the magnetically induced particle velocity, Eq. (11), can be succinctly stated as:

$$\mathbf{u}_{\mathrm{m}} = m\mathbf{S}_{\mathrm{m}} \tag{14}$$

Thus we have defined the magnetophoretic mobility by Eq. (12), and the magnetic force field strength by Eq. (13). Note that such a definition of the magnetophoretic mobility meets the criterion of being constant for linearly polarizable media (for which the magnetic susceptibility χ is constant). Such media include paramagnetic and diamagnetic substances. Also, note that for the nonlinear media, such as ferromagnetics, the magnetophoretic mobility depends on the field properties in exactly the same way as the magnetic susceptibility does [see Eq. (12)]. In such instances the value of $\Delta\chi$ can be substituted by the ratio of $\Delta M/H$ in Eq. (12).

We retained the units of $m^3\,T^{-1}\,A^{-1}\,sec^{-1}$ of the magnetophoretic mobility to emphasize its magnetoquasistatic origins (here we use the International System of Units, or SI Units, where m is meter, A is ampere, T is tesla, and sec is second). When reduced to the fundamental SI units, the unit of the magnetophoretic mobility is $m^3\,kg^{-1}\,s$ (χ is dimensionless).

The fundamental role of the magnetophoretic mobility in determining the separation parameters of a transport process is emphasized in expressions for the resolving power, X, and the throughput, Z, of the continuous flow separation process in an annular channel, located coaxially with an open-gradient magnetic quadrupole field:[16]

$$X = \frac{m_1}{\Delta m} = \frac{I_1[\rho_i, \rho_{OSC}]}{I_1[\rho_i, \rho_{ISC}]} \tag{15}$$

and

$$Z = 2\pi L \frac{B_0^2}{\mu_0} m_1 c \frac{I_2[\rho_i, \rho_{ISC}]}{I_1[\rho_i, \rho_{ISC}]} \frac{\Delta m}{m_1} \tag{16}$$

where the geometry of the system is shown in Fig. 1, and m_1 and $m_1 + \Delta m$ are characteristic magnetophoretic mobilities of the separands. The integrals I_1 and I_2 are functions of the internal to external cylinder radius ratio, ρ_i, and the flow conditions, determined by the reduced inlet and outlet splitting cylinder radii, ρ_{ISC} and ρ_{OSC}, respectively. The expressions for I_1 and I_2 are provided in Appendix A. The splitting cylinders are flow stream-surfaces that originate at the inlet flow splitter (ISC) or terminate at the outlet flow splitter (OSC) and together determine the minimum distance that the particle must travel along the (radial) direction of the magnetic force, across the flow, in order to be separated, Fig. 1. Because of it, the volume enclosed by ISC and OSC is referred to as the "transport lamina." The derivation of the integral functions I_1 and I_2 can be found in the original publication in Ref. [16]. The other parameters entering the above expressions are the length of the annular channel, L, the maximum field intensity at the outer cylinder of the annulus, B_0, and the particle number concentration, c.

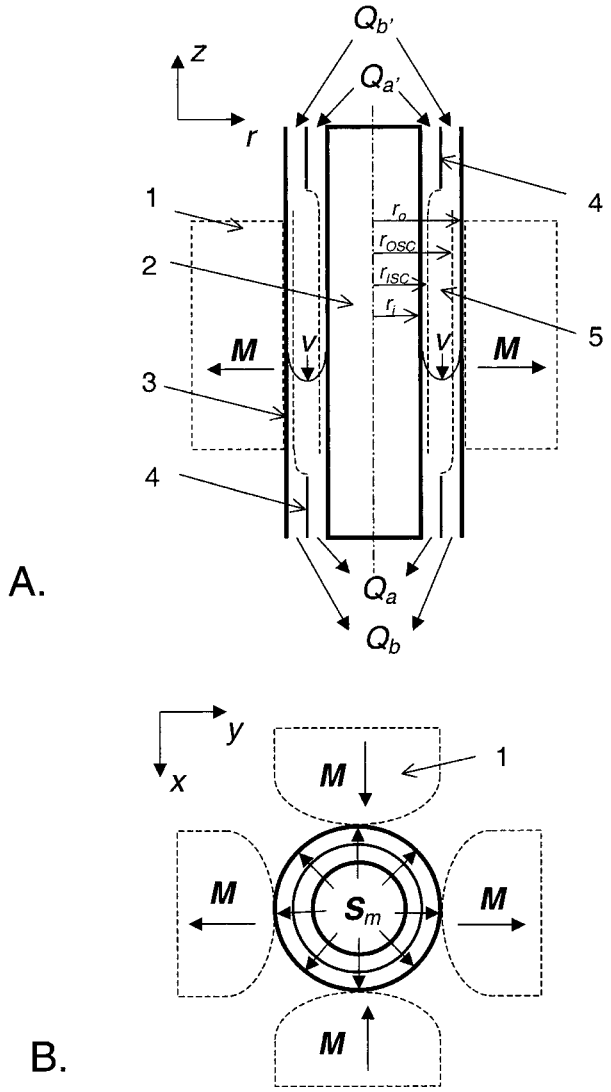

Figure 1. Quadrupole magnet flow sorter schematics. (A) Longitudinal section. 1: Permanent magnets showing directions of magnetization vectors **M**. 2: Center solid core. 3: Annular channel of outer wall radius r_0 and inner wall radius r_i showing fluid flow velocity profile, v. 4: Inlet and outlet flow splitters. 5: Transport lamina enclosed by inlet splitting cylinder stream-surface of radius r_{ISC}, and outer splitting cylinder stream-surface of radius r_{OSC}. Here $Q_{a'}$, $Q_{b'}$, Q_a, and Q_b denote volumetric flow rates which control the transport lamina thickness and position. The sample was fed into the stream $Q_{a'}$. (B) Cross-section.

From the previous expressions it is immediately obvious that the separation of separands differing little in the magnetophoretic mobility (small Δm) requires high resolving power and a low throughput (note that the throughput is inversely proportional to the resolving power). On the other hand, large difference in the mobilities of the separands allows for relaxing the requirement imposed on the resolving power and leads to high throughput. What perhaps is less obvious is that one may select the cut-off mobility by suitable selection of the size and the position of the transport lamina within the volume of the annulus, as discussed at length in the original publication in Ref. [16]. The above formulas provide quantitative relationships between the particle mobility and the magnetic separation parameters, and provide a firm basis for a systematic study of the magnetic separation processes.

Another incentive for studying the magnetophoretic mobility is its relationship to cell biology. We have shown that the magnetophoretic mobility of a magnetically labeled cell is directly proportional to the expression of characteristic molecules on its surface (typically referred to as cell surface markers, or cell surface antigens):

$$m = \frac{\phi_m}{f}\beta\,\mathrm{ABC} = \frac{\Delta\chi V_m}{3\pi\eta D_c}\beta\,\mathrm{ABC} \tag{17}$$

where V_m is the volume of each of the magnetic particles attached to the cell that impart the magnetophoretic mobility, ABC is the antibody-binding capacity of the cell, and β is the ratio of the number of magnetic particles attached to the cells and the ABC.[22–24] The above formula applies to magnetic particles that are much smaller than the cell (the magnetic particle diameter on the order of 0.1 μm as compared to a characteristic cell diameter on the order of 10 μm). A comparison of the above three formulas, Eqs. (15)–(17), clearly indicates the potential usefulness of the magnetic quadrupole flow sorting process to separate cells differing by their ABC, based on differences in their magnetophoretic mobility. A review of formulas describing the special cases of the magnetophoretic mobility is given in Appendix B.

MATERIALS AND METHODS

Magnetophoretic Mobility Measurements by Cell Tracking Velocimetry

The current cell tracking velocimetry (CTV) system is built around a magnet that produces a nearly constant S_m within the field of view of a microscope (Fig. 2). In this respect, the current CTV system is significantly different from

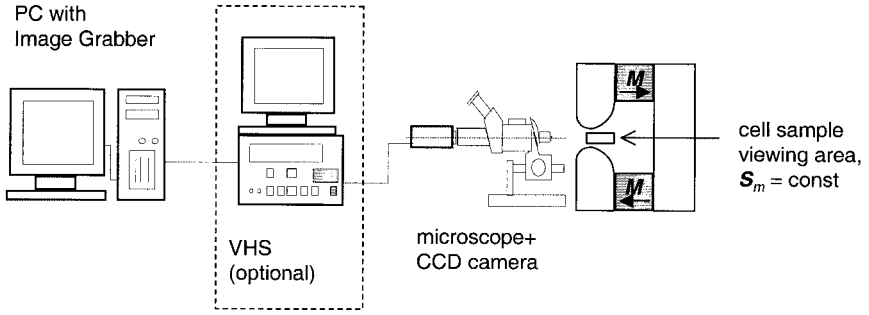

Figure 2. Cell tracking velocimetry schematics. The front end of the system is a specially designed permanent magnet assembly producing a constant energy gradient, $\mathbf{S}_{\mathrm{m}} = \text{const.}$ in the microscope's viewing area. Here the microscope is depicted in side view and the magnet in front view for illustration (not to scale).

other magnetophoresis analyzers, in which S_{m} varied rapidly with spatial coordinates,[2,5,20,25] or from an earlier version of the CTV in which S_{m} depended strongly on the particle coordinate.[26] The advantage of our current system is that it produces a constant magnetic migration velocity u_{m}, Eq. (14), over the entire viewing area, with the resulting improved resolution and accuracy of the particle velocity determination. It also allows for an accurate calculation of the magnetophoretic mobility because the value of S_{m} can be accurately determined. The current prototype is based on permanent magnets, resulting in a single value of S_{m}, however, we are in the process of implementing an electromagnet, which will allow us to vary the value of S_{m}, and thus extend the range of the analysis. The CTV analysis area is approximately $1\,\mathrm{mm} \times 1.5\,\mathrm{mm}$ for which the field varies from 1.42 to 1.71 T, the gradient varies from 196 to 161 T/m, with the resulting value of S_{m} staying nearly constant ($\pm 0.8\%$): $S_{\mathrm{m}} = 552\,\mathrm{T^2/m}/2\mu_0 = 219 \times 10^6\,\mathrm{T\,A/m^2} = 219 \times 10^6\,\mathrm{J/m^4}$. (The corresponding value of S_{m} in em cgs units is $S_{\mathrm{m}} = 276\,\mathrm{MG\,Oe/cm}$ where $1\,\mathrm{MG} = 10^6\,\mathrm{G}$, and G stands for gauss and Oe for oersted.) The details of the magnetic field geometry inside the separation element of the CTV system have been published elsewhere.[27,28]

The micrometer-size objects (particles or biological cells) migrating in the magnetic field are observed with a 5× microscope objective and a 2.5× photo eyepiece. Light is supplied internally through the objective (epi illumination). A Cohu (San Diego, CA) charge-coupled display (CCD) camera operating at a frame speed of 30 Hz, and a Sony SVO-9500 MD S-VHS (Sony Corp., Tokyo, Japan) video recorder are used to record cell movement. A μ-Tech Vision 1000 PCI Bus Frame Grabber (MuTech Corp. Billerica, MA) is used to convert the analog VCR image into a 640×840 pixel array, where each pixel contains eight bits of gray-level information ranging from 0 (black) to 255 (white). The number

of frames skipped between those which are acquired is user controlled, and depends on the particle speed. An SVGA graphics card with 800×600 resolution and 256 gray levels, and the CTV computer algorithm are used for PC-video display. Recently, we implemented a direct image acquisition from the CCD camera to the computer memory (without the intermediate step of video recording), which substantially increased the speed of image acquisition and analysis.

The particle tracking and velocity calculation are performed using a computer algorithm adapted from three-dimensional particle tracking velocimetry. It consists of two parts: determination of particle location and two-dimensional tracking. Particle locations are identified by the contrast between the object and the background, set by the user. The particles are defined by the user-selected parameters of aspect ratio, and minimum and maximum size. The particle identification and location algorithm scans the image pixels, identifies the particles, and locates their centers. The two-dimensional tracking module uses a sequence of five frames to establish the most probable path taken by the particles. The tracks are determined based on the concept of path coherence: cell position, velocity, and acceleration are internally self-consistent and can be described by smooth functions. The output of CTV gives location and velocity data, for multiple particles, over the observed frames. These velocities, combined with the known magnetic energy gradient, S_m, give magnetophoretic mobilities, using Eq. (14). When the number of particles studied is sufficiently high (at least several hundred for a narrowly dispersed sample), magnetophoretic mobility histograms are generated, from which useful statistics can be derived.

The CTV computational algorithm has been extensively tested for self-consistency and sensitivity using monodisperse magnetic particles.[29] The CTV system has also been tested for consistency with the particle susceptibility measurements using a magnetometer.[28]

Mobility-Based Separations in Quadrupole Magnet Flow Sorter

The separation element of the quadrupole magnet flow sorter (QMS) separator consists of two concentric cylinders (the inside cylinder is solid) surrounded by four pole pieces generating the magnetic quadrupole field, as shown in Fig. 1. Quadrupole magnet flow sorter inlets and outlets are connected to the QMS separation element by suitable flow manifolds, equipped with inlet and outlet flow splitters, respectively. The source of the magnetomotive force are four pieces of neodymium–iron–boron (Nd–Fe–B) permanent magnets (Dexter Magnetics Corp., Toledo, OH, maximum energy product of 40 MG Oe). The quadrupole field geometry is achieved by using four, specially shaped soft iron pole pieces adjoining the permanent magnets. The magnetic force field strength,

S_m, inside the quadrupole field is axially symmetric:[16]

$$S_m = \frac{B_0^2}{\mu_0 r_0}\rho \tag{18}$$

where $\rho = r/r_0$ is the dimensionless radial distance from the quadrupole field axis, r is the distance from the field axis, r_0 is the outer cylinder inner wall radius, and B_0 is the magnetic field at the outer cylinder inner wall (at $\rho = 1$). The numerical values of QMS parameters are: maximum field, $B_0 = 1.344\,\mathrm{T}$, $L = 76.2\,\mathrm{mm}$, $r_0 = 4.53\,\mathrm{mm}$, $r_i = 2.38\,\mathrm{mm}$, inlet flow rate ratio, $Q_{a'}/Q = 0.1$, outlet flow rate ratio, $Q_a/Q = 0.2$, total flow rate, $Q = Q_{a'} + Q_{b'} = Q_a + Q_b = 20\,\mathrm{mL/min}$ (see Fig. 1 for notation). Note that the force field strength inside the quadrupole field has a centrifugal character, i.e., it is a linear function of the distance from the field's axis of symmetry, and there are no tangential or axial components of the force strength. In particular, $S_m = 0$ at the symmetry axis of the channel, and $S_m = 317 \times 10^6\,\mathrm{J/m^4}$ (398 MG Oe/cm) at $\rho = 1$. The details of the magnetic field geometry inside the separation element of the QMS channel were published elsewhere.[30,31]

The magnetic field in the QMS separation element is the source of the radial movement of the magnetically labeled cell:

$$u_m = mS_m = m\frac{B_0^2}{\mu_0 r_0}\rho \tag{19}$$

where the cell velocity induced by the magnetic field, u_m, was obtained by combining Eqs. (14) and (18). Because of the distributed character of the CD34 cell magnetophoretic mobility, m, the radial cell velocity, u_m, was also distributed for any given ρ in the magnetic field accessible to cells. In consequence, in calculating the retrieval factors at outlets a and b, we used sets of trajectories corresponding to different mobilities, with weighting factors equal to the mobility frequency as measured by the CTV. An additional source of the distribution of the cells between the outlets a and b was the distribution of cell initial radial position when entering the magnetic field region. The combination of the radial (magnetic) and axial (convective) velocity components determined the position of the cell in the fluid stream at the outlet flow splitter, and therefore the cell assignment to either outlet a or b. The particle distribution between outlets a and b was calculated on the basis of the distribution of their magnetophoretic mobilities measured by CTV, and was verified experimentally by pulse injections of magnetic calibration particles and magnetically labeled cells into the QMS system.[32,33] A very good agreement was obtained indicating that the particle (or a cell) mobility is a reliable predictor of separation in the QMS system. Those studies led to the development of a QMS system for fast sorting of human hematopoietic progenitor cells from white blood cell population.[34]

RESULTS

A compound image of momentary particle positions taken at equal time intervals in the CTV field of view is shown in Fig. 3A. Slower moving particles can be distinguished from the faster moving ones by the closer spacing of the particle images. Note constant velocities of the particles along their respective trajectories, as indicated by equal distances between the particle positions, a result of the constant S_m in the field of view [Eq. (14)]. The particle trajectories are slightly divergent ($\mathbf{S}_m$ is pointed from right to left of Fig. 3A) indicating that the $\mathbf{S}_m$ vector (or the gradient of magnetic energy density) has a nonzero component across the CTV viewing area (along the Y coordinate, bottom to top of Fig. 3A). The particles used in that experiment were monodisperse, composite polymeric particles consisting of a polystyrene core and layers of magnetite/maghemite and silica to ensure uniformity of size and magnetic susceptibility (diameter 5.2 μm, susceptibility $\chi = 2.56 \times 10^{-3}$, obtained through a collaboration with Prof. S. Margel, Bar-Ilan University, Israel). The total number of particle trajectories analyzed in that experiment was 1131, the mean particle mobility was 1.02×10^{-3} mm^3/T A sec. The particle mobility histogram is shown in Fig. 3B.

The CTV analysis was applied to compare magnetophoretic mobilities of cells before and after tagging with a magnetic colloid used for magnetic cell separation, Fig. 4A and B, respectively. A scale with the absolute cell velocities was added for reference. The untagged cells were effectively motionless, with the mean magnetophoretic mobility of $m = 2.5 \times 10^{-6}$ mm^3/T A sec, corresponding to the mean cell velocity of 0.2×10^{-3} mm/sec $= 0.2$ μm/sec, or approximately 1/50 cell diameter a second. This low value of cell mobility is at the lower limit of the CTV resolution.[29] The mobility of the magnetically tagged cells was over 20-fold higher than that of the untagged cells, at 60×10^{-6} mm^3/T A sec, corresponding to the mean cell velocity of 4×10^{-3} mm/sec, or approximately one-half a cell diameter per second. The cells used for the experiment were white blood cells isolated from human umbilical cord blood (as approved by the OSU Institutional Review Board). The white blood cell fraction was isolated from the whole blood by density centrifugation (Ficoll-Hypaque, Accurate Chemicals, Westbury, NY) and resuspended in phosphate-buffered saline solution for CTV analysis. A cell aliquot was labeled with an antibody specific for the hematopoietic (blood-forming) progenitor cells, characterized by the presence of a complex of differentiation 34 (CD34) molecule on their surface (mouse anti-human CD34 monoclonal antibody, hapten-conjugated, Miltenyi Biotec, Auburn, CA), followed by labeling with an anti-hapten antibody conjugated to 50 nm magnetic particles (Miltenyi Biotec). The cell labeling technique targets the hematopoietic progenitor cells and magnetizes the cells by attaching small (50 nm nominal diameter) magnetic particles to their surface. The progenitor

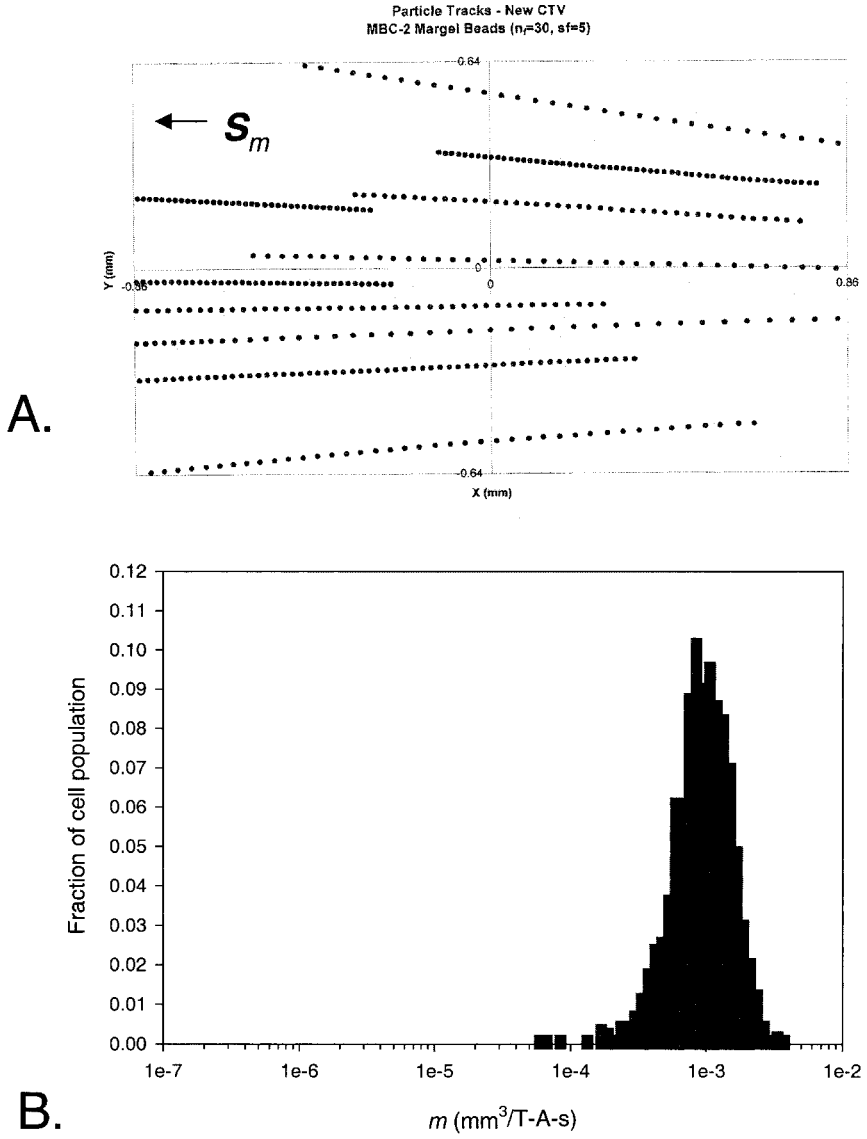

Figure 3. A sample CTV result. (A) A composite image of particle positions in the microscope's viewing area captured at equal time intervals. Note the generally uniform particle motion, and a distribution of particle velocities as indicated by differences in intervals between particles momentary positions for different trajectories. (B) Magnetophoretic mobility histogram.

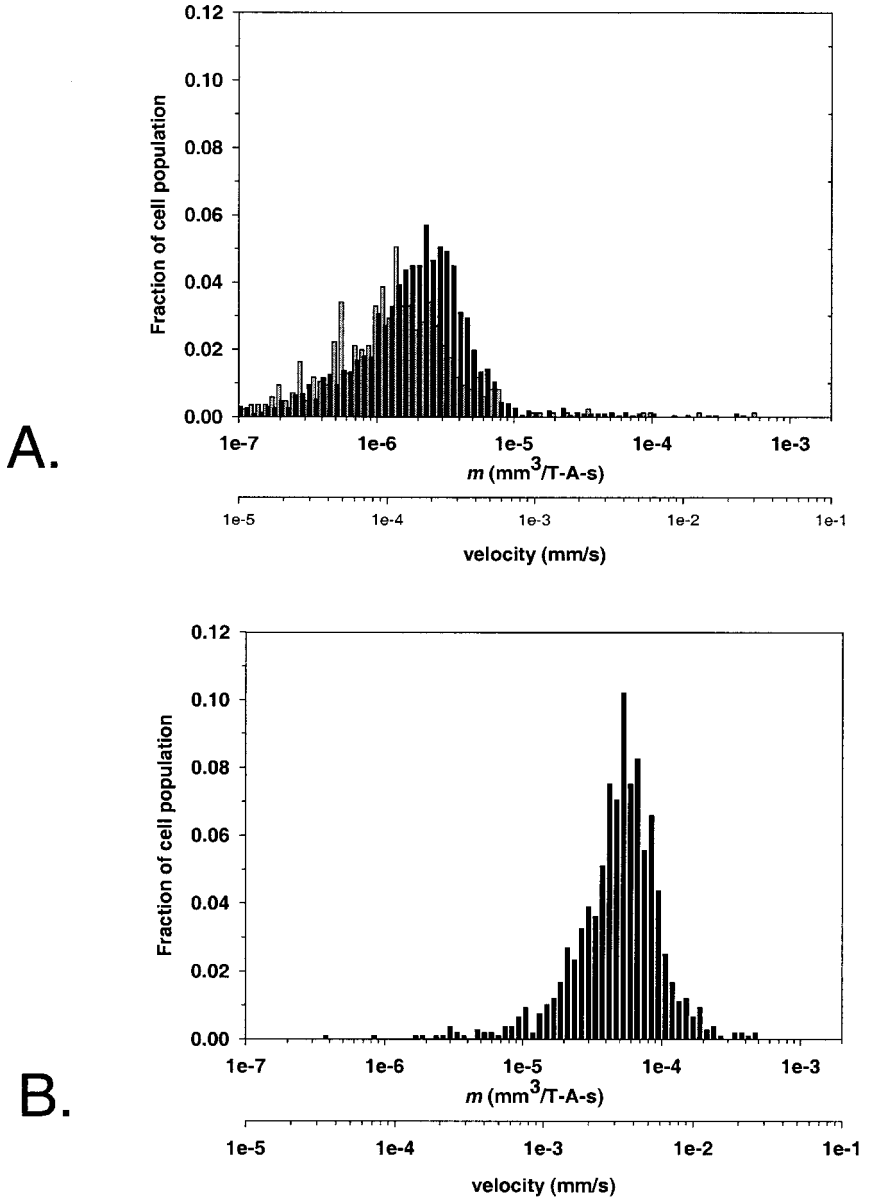

Figure 4. Magnetophoretic mobility of blood progenitor cells measured by the CTV. (A) An unlabeled cell sample. (B) A magnetically labeled cell sample using anti CD34 monoclonal antibody and a magnetic colloid. Note the significant increase in mobility of the magnetically labeled cells.

cells were enriched with a MiniMACS magnetic column prior to CTV analysis (Miltenyi Biotec).

A mixture of the magnetized and the nonmagnetized (unlabeled) cells was injected into the QMS separation system and the separated cell fractions were analyzed using a fluorescence-activated cell scanner (FACScan, Becton Dickinson, San Jose, CA). Here the hematopoietic progenitor cells were derived from the human bone marrow (as approved by the CCF IRB), and the primary, targeting antibody was conjugated to a fluorescein molecule (FITC) to distinguish the unlabeled cells from the magnetically labeled cells (mouse anti-human CD34 monoclonal antibody-FITC conjugate from Becton Dickinson, followed by anti-FITC antibody conjugated to the magnetic nanobead from Miltenyi Biotec). The results of the separation are displayed as dot plots in Fig. 5 with the accompanying statistics. The feed fraction consists of two cell populations, those that are positive for CD34 marker (Region R2) and the rest. The percent fraction of the CD34 positive cells in the feed was 5%. The CD34 positive cell population dropped to 2% in outlet a eluate and increased to 90% in the outlet b eluate, Fig. 5, as expected. Characteristically, the mean relative cell fluorescence intensity (X-Mean), which is a measure of the ABC, or the parameter ABC in Eq. (17), is high in the outlet b eluate, 270, and low in the outlet a eluate, 105, as compared to

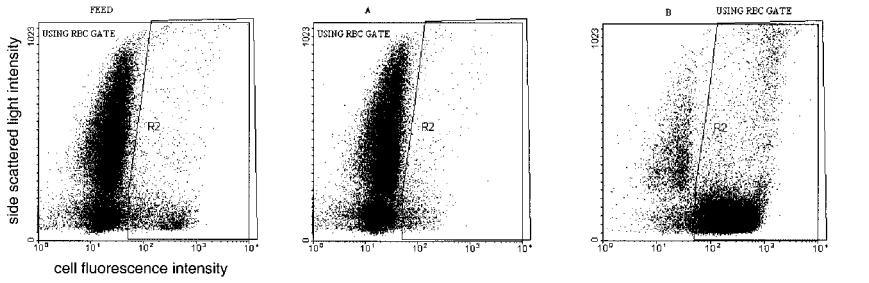

Sample: FEED
Date: 18 Jan 01
Gated Events: 93,137
System: Log Parameter
Means: Geometric

Region	X-Mean	Y-Mean	Events	%Gated
R0	26.4	378.4	93,137	100
R2	206.4	197.2	4,813	5

Sample: FRACTION A
Date: 18 Jan 01
Gated Events: 93,194
System: Log Parameter
Means: Geometric

Region	X-Mean	Y-Mean	Events	%Gated
R0	24.4	377.4	93,194	100
R2	105.2	232.6	2,012	2

Sample: FRACTION B
Date: 18 Jan 01
Gated Events: 83,038
System: Log Parameter
Means: Geometric

Region	X-Mean	Y-Mean	Events	%Gated
R0	214.8	141.1	83,038	100
R2	270.7	123.4	75,080	90

Figure 5. Dot plots and statistics of white blood cell fraction from bone marrow, by FACS. FEED: the magnetically labeled cell population injected into the QMS system in stream $Q_{a'}$. Fraction A: the cell fraction recovered in stream Q_a. Fraction B: the cell fraction recovered in stream Q_b. The blood progenitor cells were gated in the R2 region. Note the enrichment of the blood progenitor cells in fraction B as compared to the feed (90% and 5%, respectively).

that of the feed, 206 (Fig. 5). Again, this demonstrates the predictable behavior of the QMS sorting system when the results are analyzed in terms of the cell magnetophoretic mobility, and the potential of the QMS technique in sorting the cells according to their ABC.

DISCUSSION

The concept of mobility arises in describing motion of a particle driven by an external field through space filled with randomly distributed particles not responding to the field. It is also used in describing the motion of particles in continuous viscous media. It appears that there is no single definition of mobility that would encompass all different types of particle–field interactions and viscous media. Rather, such definitions tend to emphasize the particular features of the system under consideration, convenient for practical applications. For instance, the definition of the electric mobility of ions in gases is:

$$m_e = \frac{q}{m\nu} \tag{20}$$

where q is the charge of the ion, m is its mass, and ν is the collision frequency. When applied to the motion of electric charge carriers, the mobility gives rise to conductivity, defined as $\sigma = qm_e$. In the case of dielectric particle in an electrolyte solution, the electrophoretic mobility is defined as:

$$m_e \equiv \frac{Q}{f} \tag{21}$$

such that

$$\mathbf{u}_e = m_e \mathbf{E} \tag{22}$$

where Q is the net charge on the particle side of the double layer, $\mathbf{u}_e$ is the electric field-induced velocity, and $\mathbf{E}$ is the imposed electric field intensity.[35] Hence the particle charge (rather than, say, electric susceptibility times volume) plays the role of the "particle–field interaction parameter" in the electrical systems. In the theory of particle sedimentation in the gravitational or centrifugal field, the term "particle sedimentation coefficient" rather than mobility is used, defined as the ratio of particle velocity and the acceleration of the gravitational, or centrifugal, field.[37] Here the acceleration is equivalent to the force field strength and sedimentation coefficient is equivalent to mobility. Note the formal similarity between the expressions for the magnetophoretic, Eq. (12), the electrophoretic, Eq. (21), and the sedimentation mobilities. Thus, for all those different systems, the mobility is equal to particle–field interaction parameter divided by friction coefficient.[38] The units of the electric and electrophoretic mobilities are the

same (m/sec)/(V/m), but are different from those of the magnetophoretic (m/sec)/[T(A/m^2)], diffusional (m/sec)/N, and sedimentation (m/sec)/(N/kg) mobilities.

The definition of the magnetophoretic mobility adapted in our studies is compatible with the definition of the "isodynamic" magnetic field for which $\partial H^2/\partial z = \text{const.}$ on a selected plane (say, Oxz). Such a field is important in continuous magnetic separations and for magnetic particle motion analysis by CTV.[26–29] The concept of the isodynamic magnetic field, and the isodynamic magnetic separations, was introduced by Frantz in 1936, and has been the basis of commercially successful, industrial continuous magnetic sorters for separations of paramagnetic and even diamagnetic solids (by Frantz Ferrofilters Co., Trenton, NJ).[39,40]

HGMS literature introduced the definition of the "magnetic drift velocity,"[19–21] which is equal to the field-induced particle velocity, u_m, used in this article, Eq. (14). There, the "particle mobility" was defined as the ratio of the field-induced velocity and the magnetic force acting on the particle, u_m/F,[41] which is different from the particle magnetophoretic mobility, u_m/S_m, Eq. (14), as discussed in this article. The particle mobility, as used in the HGMS work, does not depend explicitly on the magnetic properties of the particle, such as its susceptibility, and in this sense has a purely Stokesian character, which sets it apart from the electric, electrophoretic, sedimentation, and magnetophoretic mobilities, as discussed here.[36]

There exists a definition of the magnetophoretic mobility that is different from the one presented earlier, namely, $m' \equiv u_m/|\nabla B|$.[2,42] Such a mobility is constant only for a special class of materials and field strengths for which the particle magnetization is constant in the field range of interest, and is convenient to use only when investigating motion of large, ferromagnetic particles in relatively small gradient magnetic fields and relatively large fields. In the light of the discussion presented previously, such an alternative definition of the magnetophoretic mobility lacks the desirable feature of being independent of field for linearly polarizable materials, and it is not directly proportional to particle susceptibility. It is also incompatible with the definition of the isodynamic fields, for which the particles of constant m' are exposed to a variable magnetic force.

The difference in mobility is the basis of separation. The topic of the importance of mobility for the rational separator design and analysis has been discussed in detail by Giddings.[14,43] Here we extend the concept of particle mobility to magnetic separations and demonstrate its usefulness in designing a novel type of magnetic separator based on a continuous, flow-through process. A combination of cell mobility determination by CTV, and the cell separation by QMS, leads to highly predictable cell separation results. We have illustrated the power of the method on the separation of the hematopoietic progenitor cells (CD34 positive cells). Currently, we extend the investigations to other cell types.

The theoretical and the experimental results provide us with a new cell separation method by which the cells are sorted on the basis of their magnetophoretic mobility.

APPENDIX A

$$I_1[\rho_1, \rho_2] = [4 \ln \rho - 2\rho^2 + 2A_2(\ln \rho)^2]_{\rho_1}^{\rho_2}$$

$$I_2[\rho_1, \rho_2] = [2\rho^2 - \rho^4 + 2A_2\rho^2 \ln \rho - A_2\rho^2]_{\rho_1}^{\rho_2}$$

where

$$\rho = \frac{r}{r_0}, \quad r_i \le r \le r_0$$

$$A_1 = (1 + \rho_i^2 - A_2)$$

$$A_2 = -\frac{(1 - \rho_i^2)}{\ln \rho_i}$$

The integrals I_1 and I_2 are related to the inlet and outlet flow rates of the QMS, $Q_{a'}$ and Q_a, and the total flow rate, Q, Fig. 1:

$$\frac{Q_{a'}}{Q} = \frac{I_2[\rho_i, \rho_{ISC}]}{A_1(1 - \rho_i^2)}$$

$$\frac{Q_a}{Q} = \frac{I_2[\rho_i, \rho_{OSC}]}{A_1(1 - \rho_i^2)}$$

The derivations are provided in Ref. [16].

APPENDIX B

Special cases of the field-induced velocity, u_m, Eq. (10), and the magnetophoretic mobility, m, Eqs. (12)–(14). The numbers in square brackets refer to the publications in the reference list, in which the particular expression was used.

1. Creeping flow around a spherical, solid magnetic particle (Stokes regime): $f = 3\pi\eta D_m$, where η is the fluid viscosity, D_m is the particle diameter, and V_m is the particle volume

$$V_m = \frac{4}{3}\pi R_m^3 = \frac{1}{6}\pi D_m^3.$$

Therefore:

$$m \equiv \frac{\phi_{\mathrm{m}}}{f} = \frac{\Delta\chi V_{\mathrm{m}}}{3\pi\eta D_{\mathrm{m}}} = \frac{2}{9}\frac{\Delta\chi R_{\mathrm{m}}^2}{\eta}$$

$$= \frac{1}{18}\frac{\Delta\chi D_{\mathrm{m}}^2}{\eta} \qquad \text{[Ref. [27], Eq. (4)]}$$

and

$$\mathbf{u}_{\mathrm{m}} = m\mathbf{S}_{\mathrm{m}} = \frac{2}{9}\frac{\Delta\chi R_{\mathrm{m}}^2}{\eta}\nabla\left(\frac{B^2}{2\mu_0}\right) \qquad \text{[Ref. [44], Eq. (2)]}$$

2. Creeping flow around a spherical magnetic shell, with the same medium inside and outside the shell.

   Supposing the shell of a diameter D_{c} comprises n discrete magnetic particles, each particle interacting with the external magnetic field with the force of magnitude F_{b}, and the parameter α denotes the particle number surface density (i.e., the particle number per unit of surface area of the shell), where:

$$\alpha = \frac{n}{\pi D_{\mathrm{c}}^2}$$

$$F = nF_{\mathrm{b}}$$

$$fu_{\mathrm{m}} = F$$

   then:

$$u_{\mathrm{m}} = \frac{F}{f} = \frac{\alpha\pi D_{\mathrm{c}}^2 F_{\mathrm{b}}}{3\pi\eta D_{\mathrm{c}}} = \frac{\alpha D_{\mathrm{c}} F_{\mathrm{b}}}{3\eta} \qquad \text{[Ref. [45], Eq. (5)]}$$

3. Supposing the number of magnetic particles comprising the shell, above, is modified by the parameter β to correct for the fact that there may not be a one-to-one binding of magnetic particles to cell surface markers, one obtains:

$$u_{\mathrm{m}} = \frac{\alpha\beta D_{\mathrm{c}} F_{\mathrm{b}}}{3\eta}$$

$$F_{\mathrm{b}} = \Delta\chi V_{\mathrm{b}}\left|\nabla\left(\frac{B^2}{2\mu_0}\right)\right|$$

$$m = \frac{u_{\mathrm{m}}}{S_{\mathrm{m}}} = \frac{\frac{\alpha\beta D_{\mathrm{c}} F_{\mathrm{b}}}{3\eta}}{\left|\nabla\left(\frac{B^2}{2\mu_0}\right)\right|} = \frac{\frac{\alpha\beta D_{\mathrm{c}}}{3\eta}\Delta\chi V_{\mathrm{b}}\left|\nabla\left(\frac{B^2}{2\mu_0}\right)\right|}{\left|\nabla\left(\frac{B^2}{2\mu_0}\right)\right|}$$

$$= \frac{\alpha\beta D_{\mathrm{c}}\Delta\chi V_{\mathrm{b}}}{3\eta} \qquad \text{[Ref. [27], Eq. (8)]}$$

4. Supposing that the total number of the magnetic particles comprising the spherical shell, above, is βABC, and that we change the notation so that $V_m \equiv V_b$, and $k \equiv \phi_m$, then: the shell–field interaction parameter $k = \Delta\chi V_m \beta$ABC, and the shell mobility:

$$m = \frac{\phi_m}{f} \equiv \frac{k}{f} = \frac{\Delta\chi V_m \beta \text{ABC}}{f}$$

$$= \frac{\Delta\chi V_m \beta \text{ABC}}{3\pi\eta D_c} \qquad \text{[Ref. [22], Eq. (11); Ref. [23], Eq. (5)]}$$

ACKNOWLEDGMENTS

These studies were supported by the grants from the NIH (R01 CA62349 to M.Z., R33 CA81662 to J.J.C.), and the NSF (BES-9731059 to J.J.C. and M.Z.).

REFERENCES

1. Hartig, R.; Hausmann, M.; Schmitt, J.; Herrmann, D.B.; Riedmiller, M.; Cremer, C. Preparative Continuous Separation of Biological Particles by Means of Free-Flow Magnetophoresis in a Free-Flow Electrophoresis Chamber. Electrophoresis **1992**, *13*, 674–676.
2. Winoto-Morbach, S.; Tchikov, V.; Mueller-Ruchholtz, W. Magnetophoresis: I. Detection of Magnetically Labeled Cells. J. Clin. Lab. Anal. **1994**, *8*, 400–406.
3. Jones, T.B. *Electromechanics of Particles*; Cambridge University Press: Cambridge, 1995; 74–82.
4. Zborowski, M. Physics of Magnetic Cell Sorting. In *Scientific and Clinical Applications of Magnetic Carriers*; Haefeli, U., Schuett, W., Teller, J., Zborowski, M., Eds.; Plenum Press: New York, 1997; 205–231.
5. Tchikov, V.; Schuetze, S.; Kroenke, M. Comparison Between Immunofluorescence and Immunomagnetic Techniques of Cytometry. J. Magn. Magn. Mater. **1999**, *194*, 242–247.
6. Zborowski, M.; Chalmers, J.J.; Williams, P.S. Magnetic FFF and Magnetic SPLITT. *Marcel Dekker Encyclopedia of Chromatography*; Marcel Dekker Inc.: New York, 2001; 503–507.
7. Melcher, J.R. *Continuum Electromechanics*; The MIT Press: Cambridge, MA, 1981; Chap. 2.
8. Ugelstad, J.; Stenstad, P.; Kilaas, L.; Prestvik, W.S.; Herje, R.; Berge, A.; Hornes, E. Monodisperse Magnetic Polymer Particles. Blood Purif. **1993**, *11*, 347–369.

9. Kantor, A.B.; Gibbons, I.; Miltenyi, S.; Schmitz, J. Magnetic Cell Sorting with Colloidal Superparamagnetic Particles. In *Cell Separation Methods and Applications*; Recktenwald, D., Radbruch, A., Eds.; Marcel Dekker: New York, 1998; 153–173.
10. Ghebremeskel, A.N.; Bose, A. Flow Through, Hybrid Magnetic Field Gradient Rotating Wall Device for Colloidal Magnetic Affinity Separations. Sep. Sci. Technol. **2000**, *35*, 1813–1828.
11. Becker, R. *Electromagnetic Fields and Interactions*; Dover Publications, Inc.: New York, 1982; Paragraph 32.
12. Schwinger, J.; DeRaad, L.L., Jr.; Milton, K.A.; Tsai, W. *Classical Electrodynamics*; Perseus Books: Reading, MA, 1998; 321.
13. Melcher, J.R. *Continuum Electromechanics*; The MIT Press: Cambridge, MA, 1981; Chapt. 3, Section 3.7.
14. Giddings, J.C. *Unified Separation Science*; John Wiley & Sons: New York, 1991.
15. Martin, M. Theory of Field Flow Fractionation. In *Advances in Chromatography*; Brown, P.R., Grushka, E., Eds.; Marcel Dekker: New York, 1998; Vol. 9, 1–138.
16. Williams, P.S.; Zborowski, M.; Chalmers, J.J. Flow Rate Optimization for the Quadrupole Magnetic Cell Sorter. Anal. Chem. **1999**, *71*, 3799–3807.
17. Dondi, F.; Martin, M. Physicochemical Measurements and Distributions from Field-Flow Fractionation. In *Field-Flow Fractionation Handbook*; Schimpf, M.E., Caldwell, K., Giddings, J.C., Eds.; John Wiley & Sons: New York, 2000; 103–132.
18. Simon, M.D.; Geim, A.K. Diamagnetic Levitation: Flying Frogs and Floating Magnets (Invited). Appl. Phys. A **2000**, *87*, 6200–6204.
19. Watson, J.H.P. Magnetic Filtration. J. Appl. Phys. **1973**, *44*, 4209–4213.
20. Takayasu, M.; Gerber, R.; Friedlaender, F.J. Magnetic Separation of Submicron Particles. IEEE Trans. Magn. **1983**, *MAG-19*, 2112–2114.
21. Bahaj, A.; Watson, J.H.P.; Ellwood, D.C. Determination of Magnetic Susceptibility of Loaded Micro-organisms in Bio-magnetic Separation. IEEE Trans. Magn. **1989**, *25*, 3809–3811.
22. McCloskey, K.E.; Chalmers, J.J.; Zborowski, M. Magnetophoretic Mobilities Correlate to Antibody Binding Capacities. Cytometry **2000**, *40*, 307–315 (Erratum. Cytometry **2000**, *41*, 150).
23. McCloskey, K.E.; Zborowski, M.; Chalmers, J.J. Measurement of CD2 Expression Levels of IFN-α-Treated Fibrosarcomas Using Cell Tracking Velocimetry. Cytometry **2001**, *44*, 137–147.
24. Schwartz, A.; Fernandez-Repollet, E.; Vogt, R.; Gratama, J. Standardizing Flow Cytometry: Construction of a Standardized Fluorescence Calibration Plot Using Matching Spectral Calibrators. Cytometry **1996**, *26*, 22–31.

25. Treat, R.P.; Lawson, W.F. Observation of Particle Trajectories Near a Magnetized Fiber. J. Appl. Phys. **1979**, *50*, 3596–3602.
26. Reddy, S.; Moore, L.R.; Sun, L.; Zborowski, M.; Chalmers, J.J. Determination of the Magnetic Susceptibility of Labeled Particles by Video Imaging. Chem. Eng. Sci. **1996**, *51*, 947–956.
27. Chalmers, J.J.; Zhao, Y.; Nakamura, M.; Melnik, K.; Lasky, L.; Moore, L.; Zborowski, M. An Instrument to Determine the Magnetophoretic Mobility of Labeled, Biological Cells and Paramagnetic Particles. J. Magn. Magn. Mater. **1999**, *194*, 231–241.
28. Moore, L.R.; Zborowski, M.; Nakamura, M.; McCloskey, K.E.; Gura, S.; Zuberi, M.; Margel, S.; Chalmers, J.J. The Use of Magnetite-Doped Polymeric Microspheres in Calibrating Cell Tracking Velocimetry. J. Biochem. Biophys. Methods **2000**, *44*, 115–130.
29. Nakamura, M.; Zborowski, M.; Lasky, L.C.; Margel, S.; Chalmers, J.J. Theoretical and Experimental Analysis of the Accuracy and Reproducibility of Cell Tracking Velocimetry. Exp. Fluids **2001**, *30*, 371–380.
30. Sun, L.; Zborowski, M.; Moore, L.R.; Chalmers, J.J. Continuous, Flow-Through Immunomagnetic Cell Sorting in a Quadrupole Field. Cytometry **1998**, *33*, 469–475.
31. Zborowski, M.; Sun, L.; Moore, L.R.; Williams, P.S.; Chalmers, J.J. Continuous Cell Separation Using Novel Magnetic Quadrupole Flow Sorter. J. Magn. Magn. Mater. **1999**, *194*, 224–230.
32. Hoyos, M.; Moore, L.R.; McCloskey, K.E.; Margel, S.; Zuberi, M.; Chalmers, J.J.; Zborowski, M. Study of Magnetic Particles Pulse-Injected into an Annular SPLITT-like Channel Inside a Quadrupole Magnetic Field. J. Chromatogr. A **2000**, *903*, 99–116.
33. Hoyos, M.; McCloskey, K.E.; Moore, L.R.; Nakamura, M.; Bolwell, B.J.; Chalmers, J.J.; Zborowski, M. Pulse-Injection Studies of Blood Progenitor Cells in a Quadrupole Magnet Flow Sorter. Sep. Sci. Technol. **2002**, *37*, 745–767.
34. Moore, L.R.; Rodriguez, A.R.; Williams, P.S.; McCloskey, K.E.; Bolwell, B.J.; Nakamura, M.; Chalmers, J.J.; Zborowski, M. Progenitor Cell Isolation with a High-Capacity Quadrupole Magnetic Flow Sorter. J. Magn. Magn. Mater. **2001**, *225*, 277–284.
35. Melcher, J.R. *Continuum Electromechanics*; The MIT Press: Cambridge, MA, 1981; Chapt. 10, Section 10.10.
36. Bird, R.P.; Stewart, W.E.; Lightfoot, E.N. *Transport Phenomena*; John Wiley & Sons: New York, 1960; 513.
37. Dhont, J.K.G. *An Introduction to Dynamics of Colloids*; Elsevier: New York, 1996; 474.
38. Dhont, J.K.G. *An Introduction to Dynamics of Colloids*; Elsevier: New York, 1996; 446.

39. Frantz, S.G. Magnetic Separation Method and Means. US Patent 2,056,426, 1936.
40. Sun, J.J. Methods and Apparatus for Separating Particles Using a Magnetic Barrier. US Patent 4,235,710, 1980.
41. Gerber, R. Magnetic Filtration of Ultra-fine Particles (Invited). IEEE Trans. Magn. **1984**, *MAG-20*, 1159–1164.
42. Schram, L.L.; Clark, B.W. On the Measurement of Magnetophoretic Mobilities. Colloids Surf. **1983**, *7*, 135–146.
43. Giddings, J.C. Field-Flow Fractionation: Analysis of Macromolecular, Colloidal and Particulate Materials. Science **1993**, *260*, 1456–1465.
44. Moore, L.R.; Zborowski, M.; Sun, L.; Chalmers, J.J. Lymphocyte Fractionation Using Immunomagnetic Colloid and Dipole Magnet Flow Cell Sorter. J. Biochem. Biophys. Methods **1998**, *37*, 11–33.
45. Chalmers, J.; Zborowski, M.; Sun, L.; Moore, L. Flow Through, Immunomagnetic Cell Separation. Biotechnol. Prog. **1998**, *14*, 141–148.

Received September 2001
Revised January 2002